[CANCER RESEARCH 64, 1094–1101, February 1, 2004]

Predictive Pharmacokinetic-Pharmacodynamic Modeling of Tumor Growth Kinetics in Xenograft Models after Administration of Anticancer Agents

Monica Simeoni,[1] Paolo Magni,[1] Cristiano Cammia,[1] Giuseppe De Nicolao,[1] Valter Croci,[2] Enrico Pesenti,[2] Massimiliano Germani,[2] Italo Poggesi,[2] and Maurizio Rocchetti[2]

[1]Dipartimento di Informatica e Sistemistica, University of Pavia, Pavia, and [2]Pharmacia Italia S.p.A., Nerviano (MI), Italy

ABSTRACT

The available mathematical models describing tumor growth and the effect of anticancer treatments on tumors in animals are of limited use within the drug industry. A simple and effective model would allow applying quantitative thinking to the preclinical development of oncology drugs. In this article, a minimal pharmacokinetic-pharmacodynamic model is presented, based on a system of ordinary differential equations that link the dosing regimen of a compound to the tumor growth in animal models. The growth of tumors in nontreated animals is described by an exponential growth followed by a linear growth. In treated animals, the tumor growth rate is decreased by a factor proportional to both drug concentration and number of proliferating tumor cells. A transit compartmental system is used to model the process of cell death, which occurs at later times. The parameters of the pharmacodynamic model are related to the growth characteristics of the tumor, to the drug potency, and to the kinetics of the tumor cell death. Therefore, such parameters can be used for ranking compounds based on their potency and for evaluating potential differences in the tumor cell death process. The model was extensively tested on discovery candidates and known anticancer drugs. It fitted well the experimental data, providing reliable parameter estimates. On the basis of the parameters estimated in a first experiment, the model successfully predicted the response of tumors exposed to drugs given at different dose levels and/or schedules. It is, thus, possible to use the model prospectively, optimizing the design of new experiments.

INTRODUCTION

A fundamental step of the preclinical development of oncology drugs is the *in vivo* evaluation of the antitumor effect. For this purpose, a series of experiments are performed, in which tumor cells from immortalized cell lines are inoculated into athymic mice. Tumor volumes are measured at different times throughout the experiment in all of the animals, treated either with a vehicle (control) or with an active drug. The effect of the active molecule is then measured by comparing the average tumor weights in treated and control animals at the end of the experiment, or by recording the animals surviving their disease (1–4). This approach can be used to select the most potent candidate within a series using the same dosing regimen, or the most appropriate dosing regimen among those tested for a specific compound. However, in this way, the time course of the tumor growth is often neglected, so that only partial use of the information available from the experiment is made.

A pharmacokinetic-pharmacodynamic (PK-PD) model, linking the administration regimen of a candidate to tumor growth dynamics, would greatly improve the preclinical development of oncology drugs. For developing this kind of model, the first step is the definition of a mathematical model describing the progression of the disease (5). A number of tumor growth models are reported in the literature, reflecting different paradigms.

Empirical models use mathematical equations (*e.g.*, sigmoid functions, such as logistic, Verhulst, Gompertz, and von Bertalanffy; Refs. 6, 7) to describe the tumor growth curve, without an in-depth mechanistic description of the underlying physiological processes. In this context, the effect of a drug can be evaluated only in terms of changes of the parameter values describing the tumor growth. Such changes depend on the dose level and the administration schedule, so that these approaches can be applied only retrospectively and not as predictive tools when used outside the tested regimens.

Functional models, conversely, are based on mechanistic, physiology-based hypotheses. They make a set of assumptions about the tumor growth, involving cell-cycle kinetics and biochemical processes, such as those related to antiangiogenetic and/or immunological responses (7, 8). Such models usually represent the cell population in its heterogeneity, splitting it into at least two subpopulations: the proliferating and the quiescent cells. More complex models describe the cell population as age-structured and take into account subpopulations related to specific phases of the cell cycle. These models have a much larger number of parameters compared with the empirical ones. Their development is time consuming and a number of quantitative observations (*e.g.*, flow cytometry analyses, biochemical and immunological marker measurements, and so forth) are required to avoid the identifiability problems due to the overparameterization. The situation becomes even more complex when the effect of the treatment with an anticancer drug is considered (9–12), also because of the incomplete knowledge of the mode of action *in vivo*. As a consequence, these models are rarely used in industrial drug research.

In conclusion, despite the existence of several tumor growth models, a practical tool that supports oncology drug development is still missing. In this respect, the only metrics of success are its application to the experimental data and the savings of experiments, time, costs, resources, and animal requirements. In this article, we describe a model that is an effective compromise between empirical and mechanism-based approaches. This model is currently used with success in the preclinical development of a number of oncology drug candidates. It relies on a few identifiable and biologically relevant parameters, the estimation of which requires only the data typically available in the preclinical setting: the pharmacokinetics of the anticancer agents and the tumor growth curves *in vivo*.

MATERIALS AND METHODS

Experimental Methods

Compounds

Paclitaxel and 5-fluorouracil (5-FU), which are commercially available; irinotecan (CPT-11), Drug A and Drug B, which have been synthesized by Pharmacia (purity, >95%), were used.

Animals

Female Hsd, athymic nude-*nu* mice, 5–6 weeks of age (20–22 g), were obtained from Harlan, S. Pietro al Natisone, Italy. Animals were maintained in cages with paper filter covers, sterilized food and bedding, and acidified water.

Received 8/14/03; revised 10/22/03; accepted 11/24/03.

The costs of publication of this article were defrayed in part by the payment of page charges. This article must therefore be hereby marked *advertisement* in accordance with 18 U.S.C. Section 1734 solely to indicate this fact.

Requests for reprints: Italo Poggesi, Pharmacia Italia S.p.A., Via Pasteur 10, 20014 Nerviano (MI), Italy. Phone: 39-02-48383172; Fax: 39-02-48385278; E-mail: italo.poggesi@pharmacia.com.

All of the animal experiments were conducted in accordance with the current best practices and ethic principles.

In Vivo Tumor Growth Experiments

A2780 human ovarian carcinoma and HCT116 colon carcinoma cell lines (from American Type Culture Collection) were maintained by s.c. transplantation in athymic mice using 20–30 mg of tumor brei. For the experiments, tumors were excised and fragments were implanted s.c. into the left flank. One week after tumor inoculation, mice bearing a palpable tumor (~100–200 mm^3) were selected and randomized into control and treated groups; tumor weight mean for all of the groups was ~0.15 g. One to 6 days after randomization (*i.e.*, from Day 8 to 13 of the experiment), the treatment with the anticancer compounds started.

Mice were clinically evaluated daily and were weighed two times weekly. Dimensions of the tumors were measured regularly by caliper during the experiments (typically from once daily to once every 4 days), and tumor masses were calculated as follows:

$$\text{Tumor weight (mg)} = \frac{\text{length (mm)} \cdot \text{width}^2\ (\text{mm}^2)}{2}\rho \qquad \text{(A)}$$

assuming density $\rho = 1$ mg/mm^3 for tumor tissue.

Drug Treatments

All of the drugs were prepared immediately before use, and treatments were given i.v. at a dose volume of 10 ml/kg.

CPT-11 (i.v. bolus) was given as a water solution to two groups of five HCT116 tumor-bearing mice; the drug was given as a single dose at the dose levels of 45 and 60 mg/kg on Day 13.

Paclitaxel (i.v. bolus) was given in two different experiments as an alcoholic solution of Cremophor (Cremophor dose, 1.2 ml/kg) starting either one day (Day 8 of experiment 1) or 6 days (Day 13 of experiment 2) after randomization. In both cases, the drug was given once every 4 days for 3 days (q4d×3) at the dose level of 30 mg/kg to groups of eight animals bearing A2780 tumors.

5-FU was given as an i.v. bolus to two groups of eight HCT116 tumor-bearing mice. The drug was given in two different experiments as a water solution at a dose level of 50 mg/kg once weekly from Day 8 either for 2 (qw×2, experiment 1) or for 4 weeks (qw×4, experiment 2).

Drug A and B are two novel anticancer candidates, part of a Pharmacia research program. Drug A was given i.v. as bolus administration starting from Day 9 of the experiment at the dose level of 60 mg/kg using three different schedules: three times daily for 1 day (tid×1), two times daily for 4 days (bid×4), and once daily for 11 days (qd×11). For each schedule, eight animals were treated. In a preliminary experiment, Drug B was given i.v. at the dose level of 15 and 30 mg/kg as bolus administration. Doses were given twice daily for 5 days (bid×5) starting from Day 13 of the experiment. Eight animals were used for each group. In a second experiment Drug B was given as a 7-day infusion (83 mg/kg/day) to 10 mice starting on Day 9 of the experiment. Experiments for Drug A and B were performed in A2780 tumor-bearing mice.

Pharmacokinetic Studies

The pharmacokinetics of CPT-11, paclitaxel, 5-FU, Drug A, and Drug B were investigated in separate groups of tumor-bearing mice (historical data from previous experiments or data obtained in small ancillary groups). Three to five animals were used for these assessments. Blood samples (~80 μl) were collected using an appropriate sampling schedule either after a single dose or before and after dosing on the last day of treatment. Blood samples were collected in heparinized tubes; the samples were immediately centrifuged at 4°C (1200 × *g* for 10 min), and plasma samples were kept at −20°C. The plasma concentrations of the drug were determined using liquid chromatographic methods with mass spectrometry detection. The lower limits of quantification were 0.25 ng/ml for CPT-11, 1 ng/ml for paclitaxel, 5.4 ng/ml for 5-FU, and 10 ng/ml for Drugs A and B.

Model Development

Pharmacokinetic Model

Plasma pharmacokinetics were described using the built-in compartmental models of Winnonlin (version 3.1, Pharsight, Mountain View, CA). Nonlinear least squares were applied using $1/y^2_{observed}$ as weighting function. For CPT-11, 5-FU, and Drugs A and B, pharmacokinetic parameters were estimated from mean drug levels. Because plasma concentration data for paclitaxel were obtained in different experiments (with the same dosing schedule but different sampling times), the pharmacokinetic analysis was performed using a naïve pooled approach.

Pharmacodynamic Model

Unperturbed Growth Model (Control Group). *In vivo* tumor growth in xenograft models is known to follow exponential growth, at least in its early phases of development (13). Subsequently, the tumor weight follows a linear growth, reaching eventually a plateau. This behavior can be described using a Gompertz model (14). Because a plateau was never observed in the experimental datasets, we preferred adopting a more flexible model focused on the exponential and linear phases. In our approach, we assumed that there is a threshold tumor mass (w_{th}) at which the tumor growth switches from exponential to linear (*i.e.*, from a first-order to a zero-order process; Ref. 15). In terms of differential equations, we have the following:

$$\begin{aligned} &\frac{dw(t)}{dt} = \lambda_0 \cdot w(t), \quad w(t) \le w_{th} \\ &\frac{dw(t)}{dt} = \lambda_1, \qquad\quad w(t) > w_{th} \\ &w(0) = w_0 \end{aligned} \qquad \text{(B)}$$

where w_0 represents the tumor weight at the inoculation time ($t = 0$), and λ_0 and λ_1 are parameters characterizing the rate of exponential and linear growth, respectively. The value w_{th} can be expressed as a function of λ_0 and λ_1, imposing the continuity of the derivatives of the model (Eq. B) at $w = w_{th}$:

$$\lambda_0 \cdot w_{th} = \lambda_1 \qquad \text{(C)}$$

From a mechanism-based perspective, λ_0 and λ_1 may be indicative of the aggressiveness of the cell line in the *in vivo* experiment and of the response of the animal (immunological, antiangiogenic, and so forth) to the tumor progression, respectively.

A model such as that described by Eq. B and Eq. C adequately describes the tumor growth in control animals (15). However, for computational reasons, it is convenient to use a single differentiable function, especially in view of the subsequent introduction of the effect of an anticancer agent (see "Perturbed Growth Model"):

$$\begin{aligned} &\frac{dw(t)}{dt} = \frac{\lambda_0 \cdot w(t)}{\left[1 + \left(\frac{\lambda_0}{\lambda_1} \cdot w(t)\right)^{\Psi}\right]^{1/\Psi}} \\ &w(0) = w_0 \end{aligned} \qquad \text{(D)}$$

For values of Ψ large enough, Eq. D is a good approximation of the original switching system. In fact, as long as the tumor weight $w(t)$ is smaller than w_{th}, the term $\{(\lambda_0/\lambda_1) \cdot w(t)\}^{\Psi}$ in the denominator is negligible compared with 1; thus, the growth rate is approximated by $\lambda_0 \cdot w(t)$ (exponential growth). On the contrary, when the tumor weight $w(t)$ becomes larger than w_{th}, 1 can be neglected, so that the growth rate becomes equal to λ_1 (linear growth). In practice, in our experience, the value $\Psi = 20$ allows the system to pass from the first-order to the zero-order growth sharply enough, as in the original switching model.

Perturbed Growth Model (Treated Groups). Whereas in the unperturbed model, all tumor cells are assumed to be proliferating, the perturbed growth model assumes that the anticancer treatment makes some cells nonproliferating (see Fig. 1), eventually bringing them to death. For a given time t, let $x_1(t)$ indicate the portion of proliferating cells within the total tumor weight $w(t)$ and let $c(t)$ indicate the plasma concentration of the anticancer agent. The growth

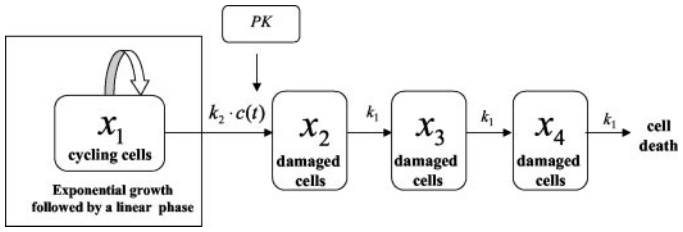

Fig. 1. Scheme of the pharmacokinetic (*PK*)-pharmacodynamic model. k_1, first-order rate constant of transit; k_2, measure of drug potency; $c(t)$, plasma concentration of the anticancer agent.

rate of proliferating cells is still given by an equation similar to Eq. D, but with $x_1(t)$ replacing $w(t)$ in the numerator, because $x_1(t)$ represents the portion of $w(t)$ that is actually proliferating. The overall tumor weight $w(t)$ in the denominator of Eq. D is maintained instead; in some sense, it acts as a penalty on the growth rate, reflecting the fact that a large tumor mass hampers the nutrient supply. The latter choice was also justified by better fitting results.

The model assumes that the drug elicits its effect decreasing the tumor growth rate by a factor proportional to $c(t) \cdot x_1(t)$ through the constant parameter k_2, which is, thus, an index of drug efficacy.

Because the death of tumor cells is delayed with respect to the drug treatment, a transit compartment model is used for describing this feature, as typically done for many signal transduction processes (Refs. 16–18; Fig. 1). It was assumed that cells affected by drug action stop proliferating and pass through n different stages (named $x_2, \ldots, x_{n+1}$), characterized by progressive degrees of damage, and, eventually, they die. The dynamics by which the cells proceed through progressive degrees of damage is modulated via a rate constant k_1 that can be interpreted in terms of kinetics of cell death. The number n of stages of damage and the value of k_1 affect the shape of the distribution of the time-to-death of damaged tumor cells. More precisely, such distribution is more bell-shaped as n grows (see Fig. 2, *left panel*). The average time-to-death of a damaged cell is equal to n/k_1, *i.e.*, it is inversely proportional to k_1 (see Fig. 2, *right panel*). In this implementation, a three-compartment transit model was considered (representing three degrees of damage), so that the model has four state variables (the proliferating portion and the three stages of damage). It is worth mentioning that, although the onset of the effect of the drug on the tumor growth curves is essentially rapid, the observable effect usually does not cease as soon as drug concentrations are negligible, because the kinetics of events in the transit compartment model may be the rate-limiting step.

The overall model can be described expressed in terms of differential equations as follows:.

$$
\begin{aligned}
\frac{dx_1(t)}{dt} &= \frac{\lambda_0 \cdot x_1(t)}{\left[1 + \left(\frac{\lambda_0}{\lambda_1} \cdot w(t)\right)^{\Psi}\right]^{1/\Psi}} - k_2 \cdot c(t) \cdot x_1(t) \\
\frac{dx_2(t)}{dt} &= k_2 \cdot c(t) \cdot x_1(t) - k_1 \cdot x_2(t) \\
\frac{dx_3(t)}{dt} &= k_1 \cdot [x_2(t) - x_3(t)] \\
\frac{dx_4(t)}{dt} &= k_1 \cdot [x_3(t) - x_4(t)] \\
w(t) &= x_1(t) + x_2(t) + x_3(t) + x_4(t) \\
&\text{with} \\
x_1(0) &= w_0, x_2(0) = x_3(0) = x_4(0) = 0 \\
&\text{and} \\
c(t) &= 0 \qquad 0 < t \leq t_0
\end{aligned}
\tag{E}
$$

In the above equations, $c(t)$ is the drug concentration (computed according to a given pharmacokinetic model) and t_0 denotes the starting time of the treatment. From time zero, when the inoculation takes place, to time t_0, start of the exposure to the drug, the tumor follows the unperturbed growth (indeed, in this time interval, $c(t) = 0$ and $x_2(t) = x_3(t) = x_4(t) = 0$, so that $w(t) = x_1(t)$).

To appreciate the effect of k_2 on the response curves, one may refer to Fig. 3, in which the simulated curves relative to different values of k_2 are plotted.

Secondary Parameters. Two important secondary parameters can be derived from the model: a time efficacy index (TEI) and a threshold concentration for tumor eradication.

TEI. If the exposure to the drug has a finite duration, when the therapeutic effect becomes negligible, the model predicts that the time course of the tumor weight will eventually follow a linear growth with slope λ_1. Thus, different treatments give rise, after a transient, to parallel straight lines, the most leftward being the one relative to the controls. In this case, the efficacy of a treatment may be measured using the delay of the tumor growth. This delay can be defined as the difference in time required to achieve a predefined tumor weight in treated animals compared with control animals during the linear growth (Fig. 4). For anticancer treatments applied to tumors in exponential growth, such a TEI can be derived with good approximation from Eq. E as follows:

$$\mathrm{TEI} = \frac{k_2 \cdot AUC}{\lambda_0} \tag{F}$$

where *AUC* is the area under the plasma concentration-time curve of the drug. Notably, in these conditions, the TEI is directly proportional to the total exposure to the drug and does not depend on the specific shape of the plasma concentration time-curve of the anticancer agent. TEI may also be determined experimentally as the tumor growth delay reported by Bissery (13).

Threshold Concentration for Tumor Eradication. For animals exposed to a steady-state drug concentration $c(t) = C_{ss}$, a threshold concentration $C_T = \lambda_0/k_2$ can be derived such that, if $C_{ss} < C_T$, the tumor will asymptotically converge to the steady-state weight $w_{ss} = \lambda_1/(k_2 \cdot C_{ss})$, which may or may not

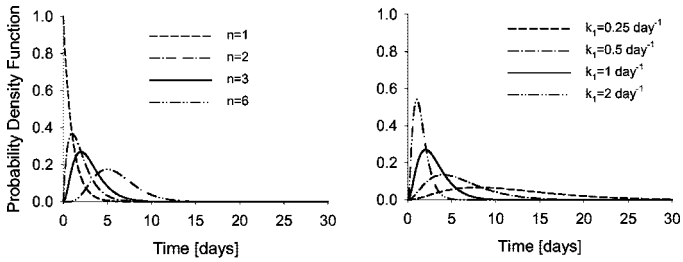

Fig. 2. Distribution of the time-to-death of tumor cells: effect of the number of compartments in the transit compartment system (*left panel*, $k_1 = 1$ day^{-1}) and of k_1 values (*right panel*; $n = 3$). k_1, first-order rate constant of transit.

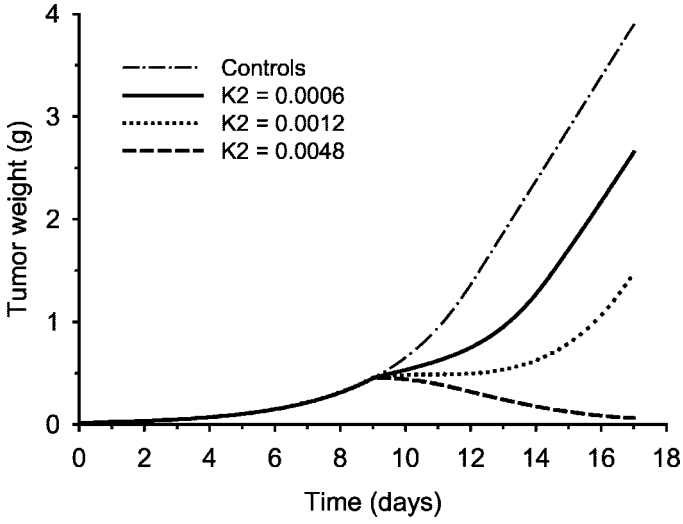

Fig. 3. Effect of k_2 on simulated tumor growth curves: the simulations were performed assuming a single i.v. bolus given on Day 9; $\lambda_0 = 0.0154$ day^{-1}; $\lambda_1 = 0.0211$ g·day^{-1}; $w_0 = 0.0162$ g; $k_1 = 0.0265$ day^{-1}. λ_0, first-order rate constant of tumor growth; λ_1, zero-order rate constant of tumor growth; w_0, tumor weight at the inoculation time; k_1, first-order rate constant of transit; k_2, measure of drug potency.

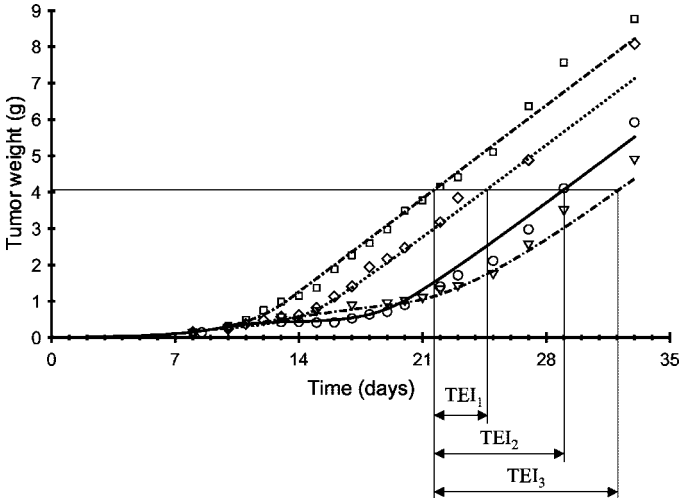

Fig. 4. Examples of measurement of the time efficacy index (*TEI*). □, Controls; ◇, treatment 1; ○, treatment 2; ▽, treatment 3.

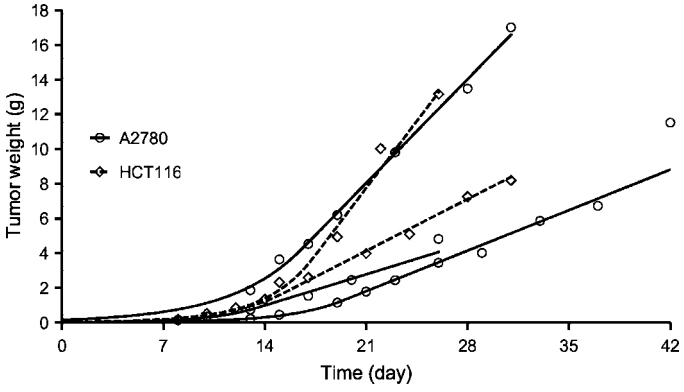

Fig. 5. Observed and model-fitted tumor growth curves in tumor-bearing nude mice (control groups) obtained in different experiments with A2780 and HTC116 cell lines.

be compatible with the survival of the experimental unit. Conversely, if $C_{ss} > C_T$, the model eventually predicts the tumor eradication independently from the weight of the tumor at the start of the treatment. This can be demonstrated based on the annihilation of the differential equations (Eq. E). It is interesting to note that C_T may be also calculated based on the experimental evaluation of TEI as *AUC*/TEI.

Data Analysis

The PK-PD model was implemented using Winnonlin (version 3.1, Pharsight). Parameters were estimated by using weighted nonlinear least squares. Different weighting strategies (uniform, $1/y_{observed}$, $1/y^2_{observed}$) were applied and chosen based on the analysis of residuals and on the coefficient of variation of the estimated parameters. Drug plasma concentrations in input to the pharmacodynamic model were derived from the pharmacokinetic parameters, using the appropriate dosing regimen. Pharmacokinetic data were obtained in separate experiments or ancillary groups, so that average pharmacokinetics were used. Also the unperturbed and perturbed tumor growth curves were obtained in different groups of animals. Therefore, model parameters were estimated by simultaneous fitting of average data of control and treated groups, which allows sharing the same tumor-related parameters w_0, λ_0, and λ_1 between the two groups.

Simulations of tumor growth curves at different doses and/or regimens were performed fixing the PK-PD parameters to their previously estimated values.

RESULTS

Unperturbed Growth Curves

The unperturbed model, with only three parameters, fitted well the average growth curves of control animals observed for different cell lines. In Fig. 5, as an example, the fitted curves are plotted against the data collected in experiments using two different tumor cell lines (A2780 and HCT116).

Perturbed Growth Curves

CPT-11. The pharmacokinetics of CPT-11 in nude mice were described using a two-compartment model; pharmacokinetic parameters after a single i.v. bolus at 45 mg/kg dose level were $V_1 = 4.85$ liter · kg^{-1}, $k_{10} = 0.553\ h^{-1}$, $k_{12} = 0.0115\ h^{-1}$, $k_{21} = 0.0616\ h^{-1}$ (model 7 of Winnonlin). Maximal concentration and plasma clearance were ~10 μg/ml and 2.7 liter · h^{-1}·kg^{-1}, respectively, consistent with the data reported in the literature (19). In Fig. 6 the fitting of the average plasma concentrations (*inset*) and the average observed and model-fitted tumor weights are shown. The PK-PD model was able to correctly describe the growth of tumors in both untreated and treated mice given a single i.v. dose of CPT-11 at 45 and 60 mg/kg dose levels ($r^2 > 0.99$). It is important to notice that the fitting of the control and treatment arms was simultaneous, which is indicative of the consistency of the parameters across the two dose levels; results are reported in Table 1.

Paclitaxel. In Fig. 7, the observed and the model-fitted average tumor growth curves are shown in control and i.v.-treated animals in two different experiments. The results of the pharmacokinetic fittings, obtained in previous experiments, are shown in the same figure. The

Table 1 *Pharmacodynamic parameters obtained fitting the model to the tumor weight data of control and treated animals*

Nude mice received i.v. either the vehicle or a single dose of CPT-11 (45 or 60 mg/kg on Day 13).

Parameter	Estimate	CV[a] (%)
k_1 (day^{-1})	0.469	22.30
k_2 (ng^{-1}·ml·day^{-1})	8.42×10^{-4}	9.43
λ_0 (day^{-1})	0.146	4.05
λ_1 (g·day^{-1})	0.334	6.67
w_0 (g)	0.085	10.01

[a] CV, coefficient of variation; k_1, first-order rate constant of transit; k_2, measure of drug potency; λ_0, first-order rate constant of tumor growth; λ_1, zero-order rate constant of tumor growth; w_0, tumor weight at the inoculation time.

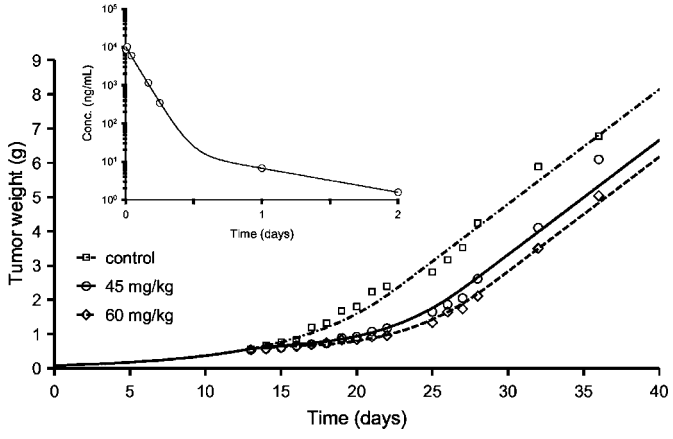

Fig. 6. Observed and model-fitted tumor growth curves obtained in nude mice given i.v. either the vehicle or a single dose of CPT-11 (*45* or *60 mg/kg* on Day 13). *Inset*, the fitting of the pharmacokinetic data of CPT-11 given as a single i.v. bolus at a 45-mg/kg dose level. *Conc.*, concentration.

Table 2 *Pharmacodynamic parameters obtained fitting simultaneously the model to the tumor weight data of two different experiments in control and treated animals*

Nude mice received i.v. either the vehicle or paclitaxel [experiment 1 (exp 1), 30 mg/kg every 4 days for 3 Days from day 8; experiment 2 (exp 2), 30 mg/kg every 4 days for 3 days from Day 13].

Parameter	Estimate	CV[a] (%)
k_1 (day^{-1})	0.968	14.53
k_2 (ng^{-1}·ml·day^{-1})	6.29×10^{-4}	8.03
λ_0 exp 1 (day^{-1})	0.273	8.08
λ_1 exp 1 (g·day^{-1})	0.814	2.34
w_0 exp 1 (g)	0.055	31.56
λ_0 exp 2 (day^{-1})	0.311	7.54
λ_1 exp 2 (g·day^{-1})	0.656	4.19
w_0 exp 2 (g)	0.033	28.17

[a] CV, coefficient of variation; k_1, first-order rate constant of transit; k_2, measure of drug potency; λ_0, first-order rate constant of tumor growth; λ_1, zero-order rate constant of tumor growth; w_0, tumor weight at the inoculation time.

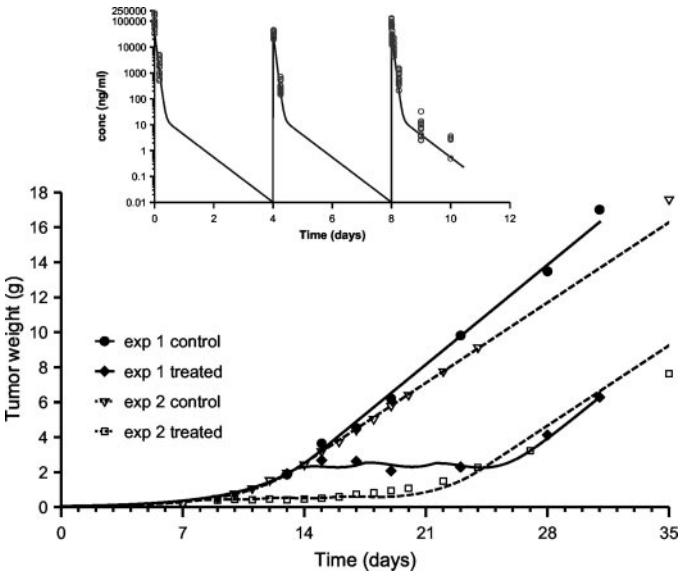

Fig. 7. Observed and model-fitted tumor growth curves obtained in two different experiments in nude mice given i.v. either the vehicle or paclitaxel [experiment 1 (*exp 1*), 30 mg/kg every 4 days for 3 days from Day 8; experiment 2 (*exp 2*), 30 mg/kg every 4 days for 3 days from Day 13]. *Inset*, the fitting of the pharmacokinetic data of paclitaxel given as repeated i.v. bolus doses at 30 mg/kg dose level; *Conc.*, concentration.

pharmacokinetics were described using a two-compartment open model (model 7 of Winnonlin). Pharmacokinetic parameters obtained after i.v. paclitaxel (30 mg/kg, every 4 days for 3 days) were $V_1 = 0.81$ liter · kg^{-1}, $k_{10} = 0.868\ h^{-1}$, $k_{12} = 0.0060\ h^{-1}$, and $k_{21} = 0.0838\ h^{-1}$. Plasma clearance was approximately 0.7 liter · h^{-1} · kg^{-1}. The comparison of these pharmacokinetics with those reported in the literature is difficult because of the known effect of Cremophor on the pharmacokinetics of paclitaxel (20); however, the shape of the curve and the maximal concentrations (~110 μg/ml) were in reasonable agreement with the values reported in the literature (20). The two experiments were performed using the same administration schedule for paclitaxel. However, the anticancer regimen were started either on study Day 8 or on study Day 13, at which times the tumor weights were ~0.2 and 2 g, respectively. The data from the two experiments were fitted simultaneously, assuming the same k_1 and k_2 across experiments. Conversely, because some differences were observed between the tumor growth in controls across experiments, different values of λ_0, λ_1, and w_0 (parameters related to the growth of control tumors) were estimated for each experiment. In Table 2, the eight pharmacodynamic parameters are reported. The simultaneous modeling captured well the features of the tumor growth and the effect of the anticancer treatment. The goodness of the simultaneous fitting ($r^2 > 0.99$) confirms the consistency of the drug-related parameters across experiments, supporting the use of the model for prediction purposes.

5-FU. An analogous evaluation, as performed with paclitaxel, was done with 5-FU, for evaluating the applicability of the model to a drug with a different mode of action. Again, two experiments were performed using the same dose levels, but, in this case, different durations of the treatments (2 and 4 weeks) were used. Observed and predicted plasma concentrations are shown in the *inset* of Fig. 8. Pharmacokinetic parameters (model 7 of Winnonlin) were $V_1 = 0.71$ liter · kg^{-1}, $k_{10} = 6.30\ h^{-1}$, $k_{12} = 0.234\ h^{-1}$, $k_{21} = 0.0964\ h^{-1}$. Plasma clearance was 4.5 liter · h^{-1} · kg^{-1}, consistent with the values obtained from the literature (21). Again, the data from the two experiments were fitted simultaneously, assuming the same k_1 and k_2 across-experiment, and different λ_0, λ_1, and w_0 for each experiment. The model captured well the features of the tumor growth and the effect of the anticancer treatment ($r^2 > 0.98$; Fig. 8). In Table 3 the pharmacodynamic parameters are reported. In this case, the large coefficient of variation of k_1 is possibly due to the nonoptimal experimental design. Parameter k_2, which is the measure of drug potency, however, was well estimated using the simultaneous fitting of all data.

Drug A. An i.v. experiment was performed with a control arm and three different dosing regimens with the active compound. To validate the within-experiment predictivity of the model, two treatment arms were intentionally omitted and the model was fitted simultaneously to

Table 3 *Pharmacodynamic parameters obtained fitting simultaneously the model to the tumor weight data of two different experiments in control and treated animals*

Nude mice received i.v. either the vehicle or 5-FU [experiment 1 (exp 1), 50 mg/kg every week for 2 weeks from Day 8; experiment 2 (exp 2), 50 mg/kg every week for 4 weeks from Day 8].

Parameter	Estimate	CV[a] (%)
k_1 (day^{-1})	0.056	212.04
k_2 (ng^{-1}·ml·day^{-1})	20.2×10^{-4}	10.98
λ_0 exp 1 (day^{-1})	0.270	10.00
λ_1 exp 1 (g·day^{-1})	1.11	5.60
w_0 exp 1 (g)	0.037	44.08
λ_0 exp 2 (day^{-1})	0.215	13.98
λ_1 exp 2 (g·day^{-1})	0.412	5.20
w_0 exp 2 (g)	0.065	48.98

[a] CV, coefficient of variation; k_1, first-order rate constant of transit; k_2, measure of drug potency; λ_0, first-order rate constant of tumor growth; λ_1, zero-order rate constant of tumor growth; w_0, tumor weight at the inoculation time.

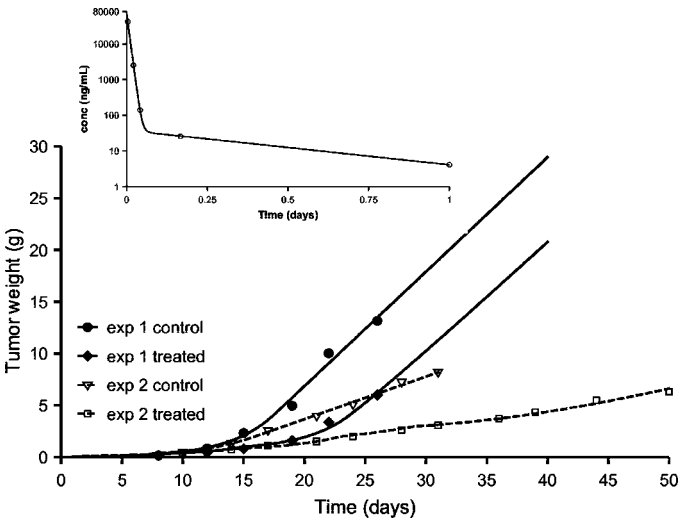

Fig. 8. Observed and model-fitted tumor growth curves obtained in two different experiments in nude mice given i.v. either the vehicle or 5-fluorouracil [5-FU; experiment 1 (*exp 1*), 50 mg/kg every week for 2 weeks from Day 8; experiment 2 (*exp 2*), 50 mg/kg every week for 4 weeks from Day 8]. *Inset*, the fitting of the pharmacokinetic data of 5-FU given as a single i.v. bolus at 50 mg/kg dose level; *Conc.*, concentration.

the data of the control arm and only one of the active treatments (the one in which 60 mg/kg was given every day for 11 days). The outcome of the pharmacokinetic fitting of the ancillary group is shown in the *inset* of Fig. 9. Plasma pharmacokinetic parameters (model 7 of Winnonlin) were $V_1 = 1.96$ liter · kg^{-1}, $k_{10} = 1.56$ h^{-1}, $k_{12} = 0.552$ h^{-1}, $k_{21} = 0.233$ h^{-1}. The results of the PK-PD modeling were excellent ($r^2 > 0.99$); the time course of the tumor weights was well described (Fig. 9), and the model parameters were estimated with good precision (Table 4). Using these parameter values and the appropriate pharmacokinetic profiles (see *inset* Fig. 10), the tumor weight curves of the two remaining treatment arms were simulated. Predicted tumor growth rates were in excellent agreement with the observations (Fig. 10). As expected, when the model was fitted to the whole dataset the results were again satisfactory ($r^2 > 0.98$) and the pharmacodynamic parameters were essentially identical to those obtained using one treatment arm only (Table 4).

The data obtained with this drug were used to validate Eq. F. In Fig. 11, the average TEI values (calculated in this case for achieving a tumor mass of 4 g) are plotted against the *AUC*; the slope of the straight line (0.0012 ml/ng) was in excellent agreement with the theoretical one ($k_2/\lambda_0 = 0.0011$ ml/ng).

Drug B. In a first experiment, Drug B was given i.v. twice a day for 5 days at the dose level of 15 and 30 mg/kg as bolus administrations. The pharmacokinetic profile obtained in a previous experiment is shown in the *inset* of Fig. 12 ($V_1 = 1.42$ ml·kg^{-1}, $k_{10} = 1.17$ h^{-1}, $k_{12} = 0.206$ h^{-1}, $k_{21} = 0.232$ h^{-1}). Pharmacodynamic parameters are shown in Table 5. The observed and model-fitted tumor growth curves are reported in Fig. 12, showing an excellent agreement ($r^2 > 0.99$). For further development of the drug, it was of interest testing the efficacy of a long-term infusion. On the basis of the λ_0 and k_2 values previously estimated, a threshold concentration for tumor eradication (C_T) of ~1100 ng/ml was calculated. An infusion experiment was designed to target a steady-state concentration of Drug B of ~2000 ng/ml (1.8-fold higher than C_T) to observe tumor shrinkage within the time frame of the experiment. On the basis of the plasma clearance obtained in the previously described experiment (1.7 liter · h^{-1}·kg^{-1}) and on basic pharmacokinetic principles (22), an infusion rate of 80 mg/kg/day was calculated: the corresponding profile is shown in the *inset* of Fig. 13. The experiment was performed at an effective infusion rate of 83 mg/kg/day: the average observed steady-state concentration was 2085 ng/ml. In Fig. 13*A*, observed and predicted tumor weights are shown, showing an excellent agreement. In Fig. 13*B* observed and model-fitted data are reported ($r^2 > 0.99$). Pharmacodynamic parameters of the infusion are also reported in Table 5. As predicted, the observed tumor weights in treated animals indeed showed the start of tumor eradication, confirming the utility of the secondary parameter C_T. This example demonstrates the across-experiments predictive power of the model using different administration modes.

Table 4 *Pharmacodynamic parameters obtained fitting the model to tumor weight data in nude mice given i.v. either the vehicle or Drug A at a dose level of 60 mg/kg*

In the left panel, the parameters refer to the fitting of controls and animals treated every day for 11 days (qd × 11) from Day 9. In the right panel, the parameters refer to the data of the whole experiment [controls, and dosages given every day for 11 days (qd × 11), twice a day for 4 days (bid × 4), three times a day for one day (tid × 1); all treatments started from Day 9].

	Controls, qd × 11		Control, qd × 11, bid × 4, tid × 1	
Parameters	Estimate	CV[a] (%)	Estimate	CV (%)
k_1 (day^{-1})	0.405	29.14	0.355	20.57
k_2 (ng^{-1}·ml·day^{-1})	3.45×10^{-4}	5.05	3.76×10^{-4}	5.27
λ_0 (day^{-1})	0.349	3.89	0.355	3.52
λ_1 (g·day^{-1})	0.363	3.60	0.366	3.47
w_0 (g)	0.010	14.77	0.009	13.08

[a] CV, coefficient of variation; k_1, first-order rate constant of transit; k_2, measure of drug potency; λ_0, first-order rate constant of tumor growth; λ_1, zero-order rate constant of tumor growth; w_0, tumor weight at the inoculation time.

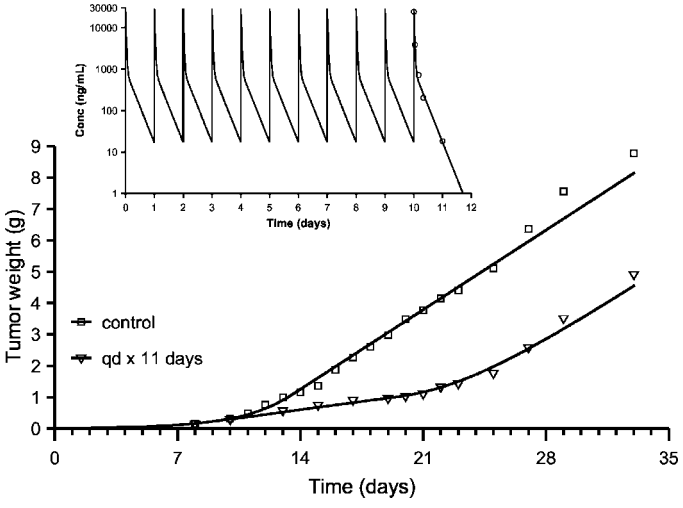

Fig. 9. Observed and model-fitted tumor growth curves obtained in nude mice given i.v. either the vehicle or Drug A [60 mg/kg every day (*qd*) for 11 days from Day 9]. *Inset*, the corresponding fitting of the pharmacokinetic data; *Conc.*, concentration.

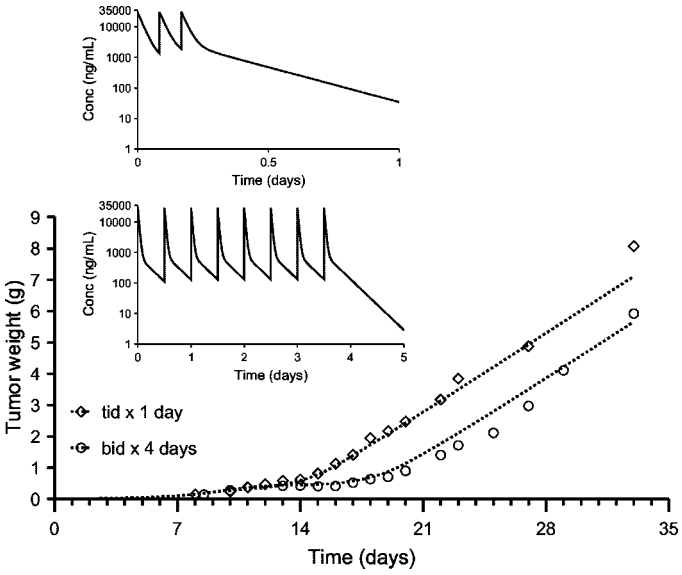

Fig. 10. Observed and predicted tumor growth curves obtained in nude mice given i.v. Drug A at 60 mg/kg dose level either three time a day for one day (*tid × 1*) or twice a day for 4 days (*bid × 4*) from Day 9. *Inset*, the simulated concentration (*Conc.*) profiles used for the predictions.

DISCUSSION

In this article, a novel PK-PD model was presented for predicting and describing the tumor growth and the effect of anticancer agents in animal models. The pharmacodynamic part of the model was based on five physiologically relevant parameters. These parameters are identifiable without additional efforts, using the typical experiments performed in nude mice as part of the drug research and development process. Three parameters (w_0, λ_0, and λ_1) describe the features of the tumor kinetics in control animals, characterized by an exponential growth followed by a linear growth. This approach was flexible enough for describing accurately the growth patterns of different cell lines in untreated nude mice (Fig. 5). It is also interesting to notice that, in its first implementation (15), the model of unperturbed growth was successfully used for modeling the tumor growth curves in rats. This flexibility is particularly important for accommodating the var-

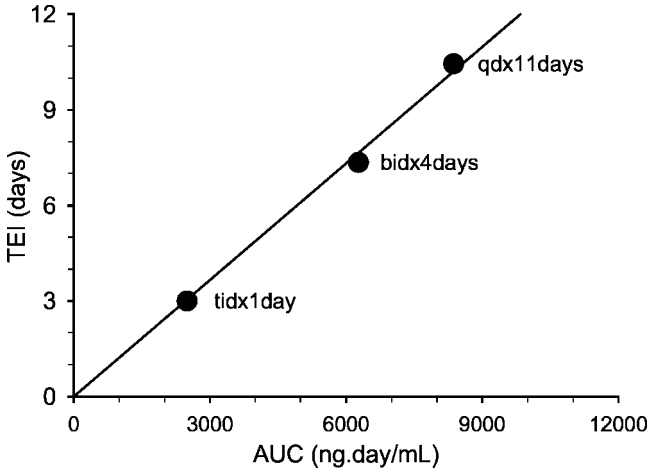

Fig. 11. Relationship between time efficacy index (*TEI*) and cumulative area under the plasma concentration-time curve (*AUC*) of Drug A for three different i.v. dosing regimens [60 mg/kg every day for 11 days (*qd ×11 days*), twice a day for 4 days (*bid ×4 days*), and three times a day for one day (*tid ×1 day*) from Day 9]. *Solid line*, the regression line passing through the origin. The slope (0.0012 ml/ng) was in excellent agreement with that calculated from Eq. F (0.0011 ml/ng).

iability observed in the average tumor growth curves of control groups. Multiple factors may cause this variability: the characteristics of the tumor implantation (number of cells inoculated and specific aggressiveness, inoculation site-specific reactions), the spontaneous response of the experimental units (immunological, antiangiogenic, and so forth), and the manipulation of the animals during the experiments. Because of this variability, metrics based solely on experimental data (*e.g.*, tumor growth inhibition) may give a different evaluation of efficacy across-experiments. In this respect, the availability of a strictly drug-specific potency parameter, independent of the growth of controls (*e.g.*, k_2 in this model), is important for a more consistent evaluation of the efficacy.

In the model of perturbed growth, the effect of an anticancer compound was related to plasma drug concentrations. It was, therefore, assumed that drug concentration in the tumor (at the target) is in rapid equilibrium with plasma (*i.e.*, the interaction with the target should not be rate limiting with respect to the kinetics of the other processes involved). In case of prodrugs or formation of active metabolites, the plasma concentrations of the active species should be used. However, in the case of irinotecan, the unchanged drug was used instead of the active SN-38 concentrations. The model was effective, however, possibly because the metabolite formation was relatively rapid and ruled by linear processes in the range of doses explored.

The effect of an anticancer compound was linearly related to both drug concentrations and tumor mass. This linear link cannot accommodate the occurrence of nonlinearities in the systems (*e.g.*, drug resistance, active or saturable processes, and so forth). Even if the anticancer effect is known to be mediated by a series of complex processes, our model was however successful in describing the response to drugs with different modes of action (topoisomerase I inhibitors, antimicrotubule assembly inhibitors, antimetabolites, inhibitors of intracellular enzymes) in a variety of different experimental conditions. A possible explanation of this robustness is that our approach does not attempt to model the specific molecular mechanism by which the tumor cells are damaged, but rather the kinetics of the damage.

The effect of an anticancer drug on the tumor weight is typically delayed and smoothed with respect to the drug exposure. For addressing this behavior, we used a transit compartmental model, a typical way to include a delay in a PK-PD model. This corresponds to a stochastic description of the events, in which the passage from one compartment to the other is assumed to be independent from what is occurring in the other compartments, and each passage is assumed to occur individually and at a uniform rate (16). A system with three compartments with a unique rate coefficient k_1 was able to generate a probability distribution of cell-death times flexible enough for accommodating all of the analyzed datasets.

The secondary parameters obtained from the model have an immediate biological meaning. The threshold concentration for tumor eradication, C_T, may be regarded as a reference concentration to be realized *in vivo* for achieving a significant activity. Only schedules able to give, at least for a certain period, concentrations higher than C_T, may have some chance to give tumor reduction. The TEI value, just as the survival time, the relapse-free survival, and so forth, is a measure of efficacy expressed in time metrics. Both C_T and TEI may be useful for extrapolating the preclinical results to humans.

The examples reported in this article referred to the modeling of average curves, which is the main goal of the exploratory studies performed in early drug discovery and development. Because of the typical features of these experiments, with separate control and treated groups and pharmacokinetics evaluated in ancillary studies, the simultaneous fitting of average data is the most efficient way for using the all of the available information. Because the perturbed growth collapses into the unperturbed one in the absence of treatment, this kind of analysis can be easily implemented with our model, validating the approach and increasing the robustness of the estimates.

Table 5 *Pharmacodynamic parameters obtained fitting the model to the tumor weight data in nude mice given i.v. either the vehicle or Drug B*

On the left, the parameters refer to i.v. bolus administrations (15 and 30 mg/kg, twice a day for 5 days from Day 13); on the right, the parameters refer to long-term i.v. infusion administrations (83 mg/kg/day, 7-day infusion from Day 9).

	Bolus		Infusion	
Parameters	Estimate	CV[a] (%)	Estimate	CV (%)
k_1 (day^{-1})	0.517	16.72	0.615	92.56
k_2 ($ng^{-1}{\cdot}ml{\cdot}day^{-1}$)	2.89×10^{-4}	9.15	2.93×10^{-4}	49.60
λ_0 (day^{-1})	0.309	22.06	0.369	3.51
λ_1 ($g{\cdot}day^{-1}$)	0.796	4.82	0.511	6.18
w_0 (g)	0.034	91.52	0.016	12.31

[a] CV, coefficient of variation; k_1, first-order rate constant of transit; k_2, measure of drug potency; λ_0, first-order rate constant of tumor growth; λ_1, zero-order rate constant of tumor growth; w_0, tumor weight at the inoculation time.

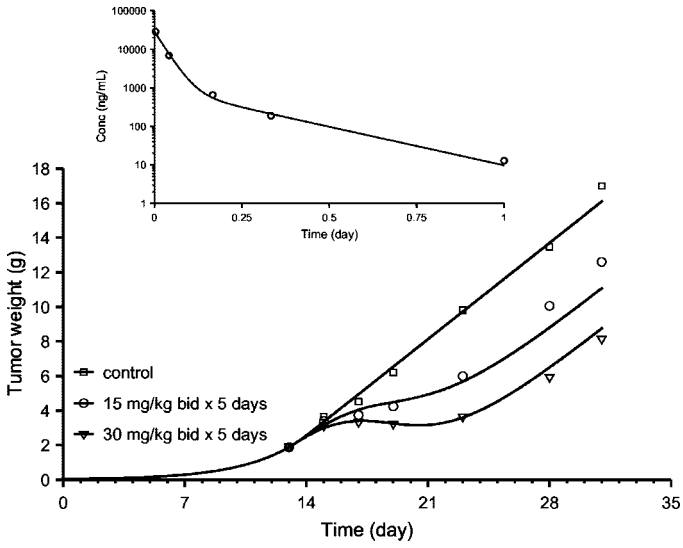

Fig. 12. Observed and model-fitted tumor growth curves obtained in nude mice given i.v. either the vehicle or Drug B [15 or 30 mg/kg, twice a day for 5 days (*bid × 5 days*) from Day 13]. *Inset*, the fitting of the pharmacokinetic data of Drug B on the last day of an every-day-for-10-days treatment at a 45-mg/kg dose level as i.v. bolus; the parameters of this fitting were used for the pharmacokinetic-pharmacodynamic modeling. *Conc.*, concentration.

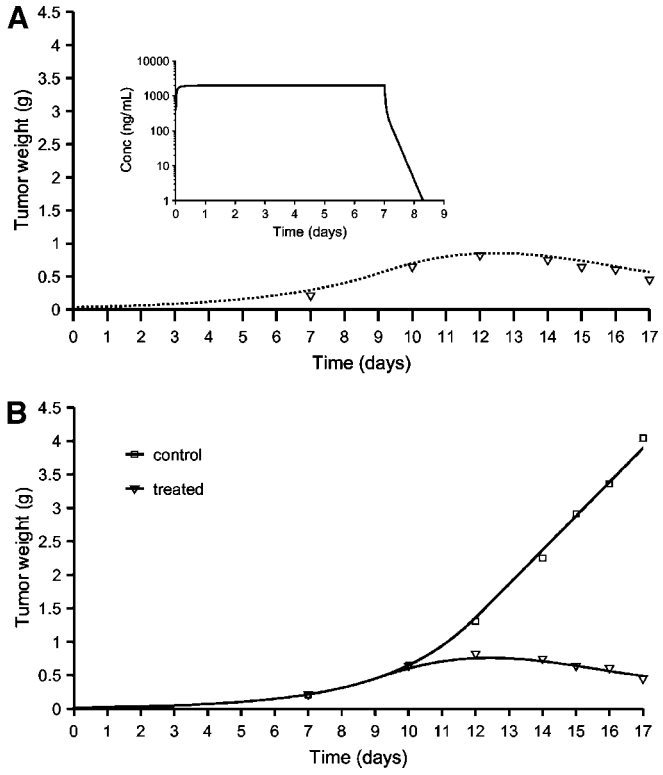

Fig. 13. *A*, observed and predicted growth curves obtained in an experiment in nude mice given Drug B as a 7-day i.v. infusion from Day 9 (dose levels: for predictions, 80 mg/kg/day; for observations, 83 mg/kg/day). *Inset*, the simulated concentration profile used for the predictions. *B*, observed and model-fitted tumor growth curves obtained in nude mice given i.v. either the vehicle or Drug B as a 7-day i.v. infusion at 83 mg/kg/day dose level from Day 9.

The examples reported on discovery candidates illustrate how this approach could expedite oncology drug discovery and development. The example concerning Drug A illustrated that, given the control and one treatment arm, the model could simulate the other two treatment arms with good accuracy. This shows that, exploiting the predictive capability of the model, a substantial simplification of the experiment is possible. In the case of Drug B, it has been shown how the model can be used for the design of subsequent experiments, identifying the appropriate dosing regimens and schedules.

In this article, we presented predictions of different dosing regimens using the same administration route. In case of changes of route, many factors can affect the response of the system (first-pass metabolism, formation of active metabolites, effect of formulations, differences in the manipulation of animals, and so forth). In such cases, caution must be exercised when the model is applied prospectively.

In conclusion, the model presented in this article correctly describes the inhibition caused by anticancer drugs with different modes of action and in different cell lines. The model has proven to be reliable enough for predicting the effect of different dosing regimens. We are currently using k_2 and k_1 estimates for ranking candidates based on their potency and for giving hints on the dynamic of cell death. The model is also being used prospectively for an educated design of the *in vivo* experiments; in this way, a number of unnecessary or less informative studies can be avoided, priority can be given to the most discriminative dosing regimens, and a more realistic evaluation of the safety margins can be obtained.

The availability of tumor growth models, achieving the right compromise between empirical and mechanism-based approaches, is also a real need in clinical practice (23). Indeed, appropriate mathematical approaches (24) may have a big impact both for driving the design of oncology trials (25–26) and for devising optimal strategies for the application of diagnostic tools in the clinics (27). The approach presented in this article may also be useful for additional considerations in this context.

REFERENCES

1. Zhang, L., Yu, D., Hicklin, D. J., Hannay, J. A. F., Ellis, L. M., and Pollock, R. E. Combined anti-fetal liver kinase. 1 Monoclonal antibody and continuous low-dose doxorubicin inhibits angiogenesis and growth of human soft tissue sarcoma xenografts by induction of endothelial cell apoptosis. Cancer Res., *62:* 2034–2042, 2002.
2. Pili, R., Kruszewski, M. P., Hager, B. W., Lantz, J., and Carducci, M. A. Combination of phenylbutyrate and 13-*cis* retinoic acid inhibits prostate tumor growth and angiogenesis. Cancer Res., *61:* 1477–1485, 2001.
3. Hammond, L. A., Hilsenbeck, S. G., Eckhardt, S. G., Marty, J., Mangold, G., MacDonald, J. R., Rowinsky, E. K., Von Hoff, D. D., and Weitman, S. Enhanced antitumour activity of 6-hydroxymethylacylfulvene in combination with topotecan or paclitaxel in the MV522 lung carcinoma xenograft model. Eur. J. Cancer, *36:* 2430–2436, 2000.
4. Fujimoto-Ouchi, K., Sekiguchi, F., and Tanaka, Y. Antitumor activity of combinations of anti-HER-2 antibody trastuzumab and oral fluoropyrimidines capecitabine/5′-dFUrd in human breast cancer models. Cancer Chemother. Pharmacol., *49:* 211–216, 2002.
5. Gieschke, R., and Steimer, J. L. Pharmacometrics: modelling and simulation tools to improve decision making in clinical drug development. Eur. J. Drug Metab. Pharmacokinet., *25:* 49–58, 2000.
6. Marušić, M., and Bajzer, Ž. Generalized two-parameter equation of growth. J. Math. Anal. Appl., *179:* 446–462, 1993.
7. Bajzer, Ž., Marušie, M., and Vuk-Pavlocić, S. Conceptual frameworks for mathematical modeling of tumor growth dynamics. Math. Comput. Model., *23:* 31–46, 1996.
8. Bellomo, N., and Preziosi, L. Modeling and mathematical problems related to tumor evolution and its interaction with the immune system. Math. Comput. Model., *32:* 413–452, 2000.
9. Sachs, R. K., Hlatky, L. R., and Hahnfeldt, P. Simple ODE models of tumor growth and anti-angiogenic or radiation treatment. Math. Comput. Model., *33:* 1297–1305, 2001.
10. Iliadis, A., and Barbolosi, D. Optimizing drug regimens in cancer chemotherapy by an efficacy-toxicity mathematical model. Comput. Biomed. Res., *33:* 211–226, 2000.
11. Miklavčič, D., Jarm, T., Karba, R., and Serša, G. Mathematical modeling of tumor growth in mice following electrotherapy and bleomycin treatment. Math. Comput. Simul., *39:* 597–602, 1995.
12. Panetta, J. C. A mathematical model of breast and ovarian cancer treated with paclitaxel. Math. Biosci., *146:* 89–113, 1997.
13. Bissery, M. C., Vrignaud, P., Lavelle, F., and Chabot, G. G. Experimental antitumor activity and pharmacokinetics of camptothecin analog irinotecan (CPT-11) in mice. Anticancer Drugs, *7:* 437–460, 1996.
14. Norton, L., and Simon, R. Growth curve of an experimental solid tumor following radiotherapy. J. Natl. Cancer Inst. (Bethesda), *58:* 1735–1741, 1977.
15. Dagnino, G., Rocchetti, M., Urso, R., Guaitani, A., and Bartošek, I. Mathematical modeling of growth kinetics of Walker 256 carcinoma in rats. Oncology, *40:* 143–147, 1983.
16. Sun, Y-N., and Jusko, W. J. Transit compartments versus γ distribution function to model signal transduction processes in pharmacodynamics. J. Pharm. Sci., *87:* 732–737, 1998.
17. Mager, D. E., and Jusko, W. J. Pharmacodynamic modeling of time-dependent transduction systems. Clin. Pharmacol. Ther., *70:* 210–216, 2001.
18. Perlstein, I., Stepensky, D., Krzyzanski, W., and Hoffman, A. A signal transduction pharmacodynamic model of the kinetics of the parasympathomimetic activity of low-dose scopolamine and atropine in rats. J. Pharm. Sci., *91:* 2500–2510, 2002.
19. Vassal, G., Boland, I., Santos, A., Bissery, M-C., Terrier-Lacombe M-J., Morizet, J., Sainte-Rose, C., Lellouch-Tubiana, A., Kalifa, C., and Gouyette, A. Potent therapeutic activity of irinotecan (CPT-11) and its schedule dependency in medulloblastoma xenografts in mice. Int. J. Cancer, *73:* 156–163, 1997.
20. Sparreboom, A., van Tellingen, O., Nooijen, W. J., and Beijnen, J. H. Nonlinear pharmacokinetics of paclitaxel in mice results from the pharmaceutical vehicle Cremophor EL. Cancer Res., *56:* 2112–2115, 1996.
21. Khor, S. P., Amyx, H., Davis, S. T., Nelson, D., Baccanari, D. P., and Spector, S. T. Dihydropyrimidine dehydrogenase inactivation and 5-fluorouracil pharmacokinetics: allometric scaling of animal data, pharmacokinetics and toxicodynamics of 5-fluorouracil in humans. Cancer Chemother. Pharmacol., *39:* 233–238, 1997.
22. Rowland, M., and Tozer, T. N. Clinical Pharmacokinetics. Concepts and Applications, Ed. 3, p. 69. Philadelphia: Lea&Febiger, 1995.
23. Piccart-Gebhart, M. J. Mathematics and oncology: a match for life? J. Clin. Oncol., *21:* 1425–1428, 2003.
24. Norton, L. A Gompertzian model of human breast cancer growth. Cancer Res., *48:* 7067–7071, 1988.
25. Hudis, C., Seidman, A., Baselga, J.,. Raptis, G., Lebwohl, D., Gilewski, T., Moynahan, M., Sklarin, N., Fennelly, D., Crown, J. P., Surbone, A., Uhlenhopp, M., Riedel, E., Yao, T. J., and Norton, L. Sequential dose-dense doxorubicin, paclitaxel, and cyclophosphamide for resectable high-risk breast cancer: feasibility and efficacy. J. Clin. Oncol., *17:* 93–100, 1999.
26. Citron, M. L., Berry, D. A., Cirrincione, C., Hudis, C., Winer, E. P., Gradishar, W. J., Davidson, N. E., Martino, S., Livingston, R., Ingle, J. N., Perez, E. A., Carpenter, J., Hurd, D., Holland, J. F., Smith, B. L., Sartor, C. I., Leung, E. H., Abrams, J., Schilsky, R. L., Muss, H. B., and Norton, L. Randomized trial of dose-dense versus conventionally scheduled and sequential versus concurrent combination chemotherapy as postoperative adjuvant treatment of node-positive primary breast cancer: first report of intergroup trial C9741/Cancer and Leukemia Group B Trial 9741. J. Clin. Oncol., *21:* 1431–1439, 2003.
27. Michaelson, J. S., Halpern, E., and Kopans, D. B. Breast cancer: computer simulation method for estimating optimal intervals for screening. Radiology, *212:* 551–560, 1999.